Noname manuscript No.
(will be inserted by the editor)

Patient-Individualized Boundary Conditions for CFD Simulations Using Time-Resolved 3D Angiography

Marco Boegel · Sonja Gehrisch · Thomas Redel · Christopher Rohkohl · Philip Hoelter · Arnd Doerfler · Andreas Maier · Markus Kowarschik

Received: date / Accepted: date

Abstract
Purpose: Hemodynamic simulations are of increasing interest for the assessment of aneurysmal rupture risk and treatment planning. Achievement of accurate simulation results requires the usage of several patient-individual boundary conditions, such as a geometric model of the vasculature but also individualized inflow conditions.
Methods: We propose the automatic estimation of various parameters for boundary conditions for computational fluid dynamics (CFD) based on a single 3D rotational angiography scan, also showing contrast agent inflow. First the data is reconstructed and a patient-specific vessel model can be generated in the usual way. For this work, we optimize the inflow waveform based on two parameters, the mean velocity and pulsatility. We use statistical analysis of the measurable velocity distribution in the vessel segment to estimate the mean velocity. An iterative optimization scheme based on CFD and virtual angiography is utilized to estimate the inflow pulsatility. Furthermore, we present methods to automatically determine the heart rate and synchronize the inflow waveform to the patient's heart beat, based on time-intensity curves extracted from the rotational angiogram. This will result in a patient-individualized inflow velocity curve.
Results: The proposed methods were evaluated on two clinical datasets. Based on the vascular geometries, synthetic rotational angiography data was generated to allow a quantitative validation of our approach against ground truth data. We observed an average error of approximately 5.7% for the mean velocity, 7.1% for the pulsatility. The heart rate was estimated very precisely with an average error of about 0.8%, which corresponds to about 6 ms error for the duration of one

Marco Boegel · Andreas Maier
Pattern Recognition Lab, Department of Computer Science, Friedrich-Alexander Universität Erlangen-Nürnberg, Martensstr. 3, 91058 Erlangen, Germany
E-mail: marco.boegel@fau.de

Sonja Gehrisch · Thomas Redel · Christopher Rohkohl · Markus Kowarschik
Siemens Healthcare GmbH, Siemensstr. 1, 91301 Forchheim, Germany

Philip Hoelter · Arnd Doerfler
Department of Neuroradiology, Universitätsklinikum Erlangen, 91058 Erlangen, Germany

cardiac cycle. Furthermore, a qualitative comparison of measured time-intensity curves from the real data and patient-specific simulated ones shows an excellent match.
Conclusion: The presented methods have the potential to accurately estimate patient-specific boundary conditions from a single dedicated rotational scan.

Keywords angiography · computational fluid dynamics · hemodynamics · cone-beam CT · flow quantification

1 Introduction

In recent years, increasing interest has been drawn to simulating a patient's hemodynamics using CFD for classifying the risk of rupture as well as treatment planning of intracranial aneurysms. Despite a general agreement that physical quantities such as wall shear stress, pressure, blood flow velocities, etc. play a major role and CFD is becoming increasingly attractive for assessing patient-specific aneurysm hemodynamics, a reliable validation of the CFD results is required prior to applications in clinical environment.

Ford et al. first suggested the generation of synthetic, virtual angiograms based on CFD simulation results and a succeeding comparison with the corresponding angiogram representing the real patient's hemodynamics [9]. In addition, further studies focusing on simulating patient's blood flow [3, 14] as well as *in vitro* blood flow of cerebral aneurysm phantoms have been published [5, 13], where parameters, e. g. blood flow velocities in proximal vessel segments, are known.

Flow quantification is not only of diagnostic importance. It has been demonstrated recently that interventional flow quantification can leverage peritherapeutic decision making [11], as flow information may guide the determination of treatment endpoints.

In this paper, we extend methods first proposed by Endres et al. [7]. They introduced a workflow for creating multiple view virtual angiography (VA) based on discrete particle methods using the extraction of contrast agent injection information from 2D digital-subtracted angiograms (DSA) to define boundary conditions for virtual angiography. An additional synchronization of the heart state at the beginning of virtual and acquired angiographic sequences was proposed in [6].

Previous work on patient-individualized hemodynamics typically requires multiple image acquisitions, (i) a 3D rotational angiography for the geometric information and (ii) an angiographic sequence with high temporal resolution (30 fps) [6]. However, in many cases angiographic sequences are acquired only at much lower temporal resolution in order to reduce X-ray dose. One of the contributions of this extended work is an automatic parameter extraction from a single dedicated rotational scan used to compute a time-resolved 3D vascular dataset (4D DSA) [4]. Relying only on a single scan reduces the X-ray dose, as well as the amount of injected contrast medium. However, working with rotational angiography data introduces new challenges for the extraction of flow information, including vessel overlap in some view angles and the extraction of time-intensity curves from 2D projection images.

Wächter et al. proposed a similar approach for flow quantification [15]. However, their method is based on a simplified 1D lamina-based flow simulation, which

is fast to compute but difficult to apply to clinical data. They use a simplified geometric model, assuming circular vessel cross-sections and segments of constant radius. Their method was extensively evaluated on phantom data, however it proves difficult to use on clinical data due to the limitations of the vasculature model.

In this work, 3D CFD simulation is used, which can be more readily applied to clinical data, however computation is much slower. Therefore, we require different approaches to properly optimize the boundary conditions. While Wächter et al. are able to use gradient descent to optimize all parameters of their model, due to the fast evaluation of their flow model, we use different approaches to estimate the boundary conditions, to minimize the number of required CFD simulations. By analyzing the distribution of blood flow velocities in projection data from rotational angiographic image acquisition sequences covering an extended angular range of 260°, the mean velocity of the patient's blood flow is estimated and then used to define boundary conditions for CFD simulation. In addition to the automatic extraction of heart rate, heart state and injection bolus, we further introduce an iterative optimization method to estimate the pulsatile pattern of the inflow velocity using CFD and VA.

2 Patient-Individualized Boundary Conditions for CFD Simulations

This section starts by providing a short overview of the data acquisition protocol for the time-resolved 3D angiography data used in this work as well as a description of the CFD technology used to simulate the blood flow. We then shortly discuss the algorithms that were used to process the angiographic image data to extract the important flow information. Afterwards, we introduce step-by-step the patient-specific parameters and present the algorithms we used for their estimation. First, the patient-specific heart rate and the heart state corresponding to the angiography acquisition are determined. Afterwards, a statistical analysis is proposed to estimate the mean inflow velocity for the simulation. Then – using CFD and VA (Siemens Healthcare GmbH, Germany, prototype not for diagnostic use) – we present an iterative optimization approach to obtain patient-specific inflow pulsatility.

2.1 Time-Resolved 3D Angiography

While previous work required separate image acquisitions and contrast agent injections for the geometric and temporal information, in this work a single image acquisition protocol is used that yields both from one acquisition and a single injection of contrast medium [4, 8].

In order to acquire a sufficiently consistent set of projection images for the 3D reconstruction and to capture important temporal information, such as the inflow and the washout of contrast agent, a long image acquisition time is required. Our acquisition protocol acquires a set of 304 projection images over a timespan of approximately 12 seconds, corresponding to a frame rate of 30 frames per second.

During image acquisition 21 ml of undiluted contrast agent is injected into the internal carotid artery at a rate of 3 ml/s for a duration of 7 seconds. The injection

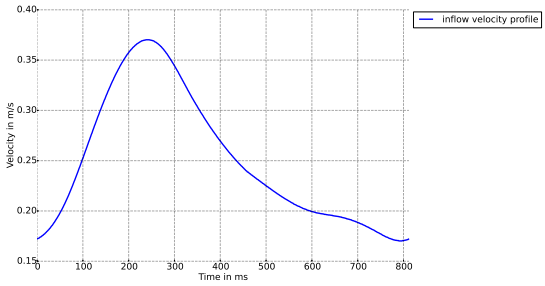

Fig. 1 Inflow velocity waveform, adapted from Karmonik et al. [12].

protocol is based on an X-ray delay of 0 seconds such that the inflow of contrast medium can be retrieved from the first subset of projection images.

2.2 Computational Fluid Dynamics

To perform pulsatile CFD simulations, a surface mesh of the vasculature with user-defined inlet and outlet boundaries is required. Thus, a 3D reconstruction of the data needs to be segmented by the user. The CFD framework then embeds this surface mesh in a Cartesian grid using a level set algorithm. In accordance with [6], blood is modeled as a Newtonian fluid with density $\rho = 1000\text{kg/m}^3$ and viscosity $\mu = 0.004\text{Pa} \cdot \text{s}$.

At the inlet, a time-varying inflow velocity profile is applied, which is modeled spatially flat. At the outlets, zero-pressure boundary conditions are assumed. In order to exclude transient effects, two cardiac cycles are simulated, while only the second cycle is stored and evaluated. The velocity waveform (see Figure 1) used in this work is adapted from the inflow velocity profile presented by Karmonik et al., which is based on 2D phase-contrast MRI measurements [12].

2.3 Virtual Angiography

VA refers to the simulation and visualization of contrast agent transport [6]. For this purpose, the propagation of mass- and dimensionless particles is simulated using the CFD-based time-varying velocity field. These particles can move freely through the vasculature. Two physical motion processes are considered. First, the particles are transported according to the velocity field. This process is called advection. In an intermediate step, the spatial distribution of the particles is employed to estimate a concentration gradient field for the simulation of diffusive flow. This diffusion process models the mixing of contrast agent and blood.

2.4 Patient-Individual Parameter Estimation

In order to estimate patient-specific inflow boundary conditions for CFD, the respective flow information first needs to be extracted from the time-resolved 3D an-

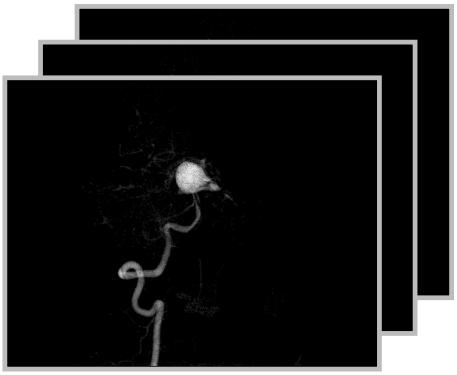

(a) Rotational angiography projection images.

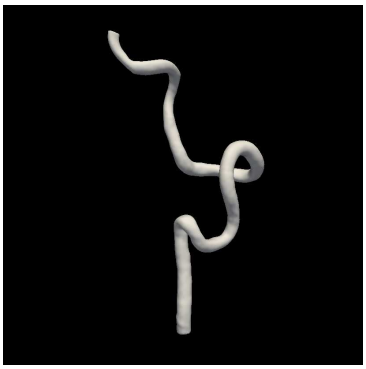

(b) Segmentation of the reconstructed 3D vessel segment.

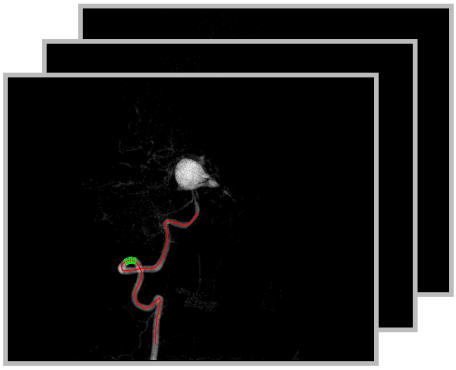

(c) Centerline and ROIs.

(d) Flow map (including reliability).

Fig. 2 The four main processing steps. 2(a) shows the sequence of rotational angiography images that were acquired. These images are tomographically reconstructed and a vessel section is segmented (2(b)). Based on the 3D image, the centerline is extracted and forward projected to each projection (2(c)). Green outlines show examples for the placed ROIs to measure time-intensity curves, which are used to extract the flow map (2(d)). Black regions in the flow map indicate unreliable sections.

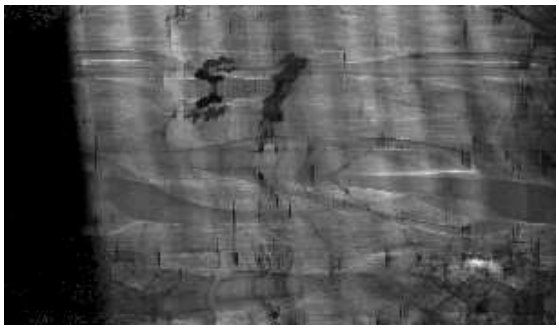

Fig. 3 Flow map of a clinical case. Each row represents a time-intensity curve measured at a centerline point.

giography projection data. Figure 2 depicts the four main steps which are needed to extract this information and are described in the following section.

We start by tomographically reconstructing the projection data as the 3D constraint volume [4]. We use a threshold-based method to obtain a first vessel segmentation [1]. As CFD simulations are computationally very demanding, we further crop the 3D volume to a smaller region containing a sufficiently long arterial segment for our estimation approach, see Figure 2(b). Then, the 3D vessel centerline is determined for this segment [10]. The centerline extraction is fully automatic and requires no further user interaction. We sample the centerline in an equidistant manner to get a set of centerline points. Subsequently, this set of centerline points is forward projected w.r.t. each projection angle of the rotational scan, resulting in multiple sets of 2D centerline points. Additionally, we determine the corresponding vessel radii for each of these points at every time step using a ray-tracing approach along the projection ray through our segmented 3D constraint volume.

It is possible to directly use the 2D centerline points to extract time-intensity curves from the acquired projection images. However, single point measurements will generally result in very noisy time-intensity curves. Instead, we propose to integrate the image intensities in relatively small region of interests (ROIs). This is done by automatically placing rectangular ROIs centered around each centerline point in the 2D projection. Each rectangle is oriented tangential to the centerline, its height is determined by the distance to the neighboring points. The rectangle width is given by the vessel radius, see Figure 2(c). Finally, we have a measurement for each centerline point for each time step (i.e., projection angle) which is normalized by the corresponding vessel radius, resulting in a time-intensity curve measured at each 3D centerline point. For visualization purposes, these time-intensity curves are arranged in a so-called flow map, as depicted in Figure 3, see also [15].

Furthermore, we need to extract the reliability $R(i,t)$ for each centerline point i at every time step t. For flow measurements we need to be aware of two problems that are especially prevalent when using rotational projection data: Overlapping vessels and foreshortening lead to unreliable measurements. Therefore, we compute the reliability map to mask the unreliable segments

$$R(i,t) = \begin{cases} 0 & \text{if overlap or foreshortening occurs} \\ 1, & \text{otherwise} \end{cases}. \tag{1}$$

To detect the overlap, we use a ray-tracing approach to count the number of vessels the projection ray corresponding to this point intersects. Foreshortened points are detected by counting the number of 3D centerline points that are projected close to this point.

Given the flow map and the reliability map of our vessel model (see Figure 2(d)), we can now estimate the patient-specific boundary conditions for a CFD simulation of this vessel segment.

Heart Rate Heart rate as a boundary condition for CFD is highly patient-specific, and as such it should be avoided to use a generalized parameters from literature. Many factors such as age or physical constitution of the patient affect the heart rate. In order to extract the patient's heart rate from the angiography data we use the time-intensity curve corresponding to the inlet of the CFD model. First,

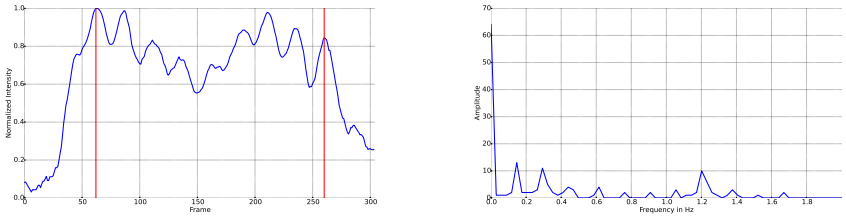

(a) Time-intensity curve (b) Fourier-transform of contrast agent plateau

Fig. 4 Time-intensity curve at the inlet of the CFD model. The contrast agent plateau is delineated in red. On the right hand side the corresponding Fourier-transform of the contrast agent plateau is shown.

we extract the contrast agent plateau from the curve by detecting the times of leading and trailing half-peak intensity. On this contrast agent plateau we detect the alternating maxima and minima and for further steps we consider only the part of the signal between the first and last detected maximum, as indicated by the red lines in Figure 4(a). This reduced signal is then zero-padded to increase frequency resolution and the Fast Fourier Transform is applied. Finally, we need to detect the dominant frequency which should correspond to the patient's heart rate. We do not consider low frequencies of less than 0.5 Hz in our search for the maximum frequency, as such low frequencies correspond to unnaturally low heart rates of less than 30 bpm. This overlying low frequency drift in the signal is likely caused by brain parenchyma enhancement.

Figure 4(a) shows an example of a time-intensity curve where the superimposed low frequency component of the signal is clearly visible. The part of the signal that was used for the Fourier Transform is delineated in red. In Figure 4(b), the corresponding frequency domain is shown, where the peak at approximately 1.2 Hz indicates the heart frequency.

Given the heart frequency, we can compute the duration of one cardiac cycle and resample the default inflow velocity profile (as depicted in Figure 1) to this time period.

Heart State Not only is the heart rate an important element in performing a patient-individual CFD simulation, we also need to determine the correct state of the heart corresponding to the start of the image acquisition. To achieve this, we use the time-intensity curve at the inflow position of our model and the velocity profile with the optimized cardiac cycle length. The velocity profile is periodically expanded to fit the duration of the rotational angiogram.

As we aim to match a velocity signal to an intensity signal, we first need to discuss the relationship between blood flow velocity and the observed intensity. High velocity means that relatively large amounts of blood are moved per time. Assuming a constant contrast agent injection rate, this leads to a relatively low contrast agent concentration and therefore low intensities are observed [2]. Our aim is to find the correct time shift Δt that ideally matches high velocity peaks of our periodic inflow velocity profile to intensity minima in the time-intensity curve. We propose the following objective function:

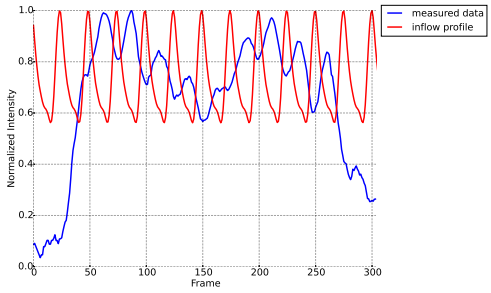

Fig. 5 Time-intensity curve at the inlet (blue). The heart rate and heart state adjusted inflow velocity profile is overlaid in red.

$$\text{argmin}_{\Delta t} \sum_{i=1}^{N} (p_{\max}(i) - v_{\min}(i) - \Delta t)^2 \cdot w_{\max}(i) + \sum_{j=1}^{M} (p_{\min}(j) - v_{\max}(j) - \Delta t)^2 \cdot w_{\min}(j), \tag{2}$$

where $p_{\max}$ and $p_{\min}$, respectively denote the time points of the N maxima and M minima in the time-intensity curve. Correspondingly, $v_{\max}$ and $v_{\min}$ represent the time positions of the velocity extrema in the periodic inflow velocity profile, respectively. Additionally, we introduced Gaussian weights $w_{\max}$ and $w_{\min}$ to give more importance to earlier time instances. Figure 5 shows the result of the heart state optimization for one example case. The measured time-intensity curve is shown in blue, while the periodic inflow velocity profile is overlaid in red.

Contrast Agent Injection Bolus We cannot directly compare the CFD results to the angiography data, as the former is given as a 4D volume of velocity vectors and the latter is a sequence of 2D projection images. Using virtual angiography, we can visualize the simulation results as projection images similar to the real data. To perform such a VA, we first need to specify the contrast agent injection bolus. We cannot simply use the time-intensity curve measured at the inlet as the injection bolus, we first need to remove the underlying pulsatile pattern. As the CFD already simulates pulsatile blood flow, using the measured time-intensity curve as injection bolus, the pulsatility would be considered twice. To solve this problem, we extract the injection bolus from the measured data by fitting a capacitor function [14, 15, 6, 13] using the Levenberg-Marquardt algorithm.

Mean Inflow Velocity A simple way to compute the mean blood flow velocity is to apply $v = \frac{\Delta s}{\Delta t}$, where Δs is the distance between two points on the 3D centerline, and Δt denotes the corresponding difference in bolus arrival time observed in the time-intensity curves. However, estimating the mean blood flow from a single measurement may not be very robust. For a reasonably accurate estimation of the mean velocity we ideally need to observe a full heart cycle. Thus, the result depends on the distance between the two selected points and the observed time interval. I.e., if the distance is too short we might only estimate the average velocity during systole or diastole, which would be an inaccurate estimate of the mean blood flow

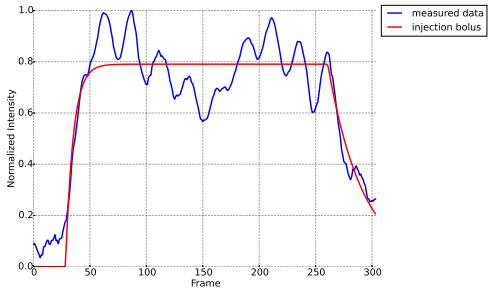

Fig. 6 Time-intensity curve at the inlet (blue). The fitted capacitor curve that is used as the injection bolus is plotted in red.

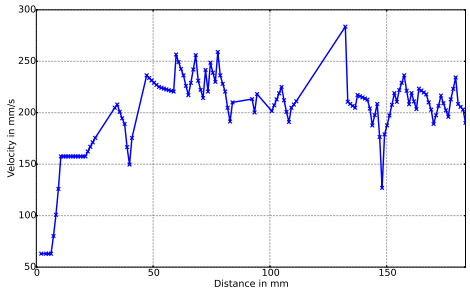

Fig. 7 Velocity measurements over different distances along the centerline. Missing measurement points correspond to unreliable centerline points.

velocity. Additionally, overlaying brain parenchyma or noise can also lead to noisy arrival times. Figure 7 depicts the problem as an example plot for a clinical case. A vessel of about 180 mm centerline length was considered. We calculated the velocity always starting from the first centerline point at the inlet and measured over increasing distances. Missing measurement points correspond to unreliable centerline points.

Instead of doing one single velocity measurement, we propose to do a more robust statistical analysis of the data. We calculate N_v velocity estimates by selecting random pairs of centerline points. If the distance between the two points is too short or one of the points is not reliable, the point pair is not considered and a new pair is drawn. Finally, we compute the mean velocity as the mean value of all N_v measurements.

Inflow Pulsatility Pulsatility describes the amplitude between the minimal and maximal velocity throughout the cardiac cycle. As previously explained, the observed contrast agent intensity is related to the blood flow velocity. Thus, due to the mixing of blood and contrast agent, we can observe the changing velocity as a pulse pattern in the extracted flow maps.

In order to determine the patient-specific pulsatility, we first need to compute a CFD simulation using the estimated parameters as described in this work. Then, a virtual angiography based on this simulation is computed using the patient-specific

contrast agent injection bolus as previously described. The virtual angiography data is forward projected using the calibration data from the original time-resolved angiography scan. Finally, we extract the virtual flow map $\widetilde{F}$ using the same method we used to extract the real flow map F from the angiography data.

Although it is theoretically possible to optimize the pulsatility directly, using a gradient-descent approach [15] to minimize the squared difference of $\widetilde{F}$ and F, such an approach requires multiple evaluations of the cost function per iteration and therefore many time-consuming CFD and VA computations.

Instead, we propose an alternative cost function that requires few iterations and can be optimized without gradient information. As a first step, the detection of all minima $p_{\min}$ and maxima $p_{\max}$ for each time-intensity curve is required. Then, for each time-intensity curve the extrema are averaged as

$$\overline{f}_{\min}(i) = \frac{1}{N_i} \sum_{j=1}^{N_i} F(i, p_{\min}(j)), \tag{3}$$

where $F(i, p_{\min}(j))$ denotes the intensity at the position of the j-th minimum in the i-th time-intensity curve and $\overline{f}_{\min}(i)$ the average observed intensity at the local minima in the i-th time-intensity curve. The number of minima in the i-th time-intensity curve is given by N_i, this number may differ between curves.

The average maximum values $\overline{f}_{\max}(i)$, and the respective virtual measurements $\overline{\widetilde{f}}_{\min}(i)$ and $\overline{\widetilde{f}}_{\max}(i)$ are computed correspondingly. We can compute the overall intensity difference between minimum and maximum values for the measured data

$$c_{\text{real}} = \sum_{i=1}^{P} ((\overline{f}_{\max}(i) - \overline{f}_{\min}(i)) \cdot r(i), \tag{4}$$

with P being the total number of time-intensity curves and $r(i)$ the average reliability of the i-th time-intensity curve. Equivalently, we can compute the overall difference between minimum and maximum intensity values for the simulated data

$$c_{\text{virtual}} = \sum_{i=1}^{P} ((\overline{\widetilde{f}}_{\max}(i) - \overline{\widetilde{f}}_{\min}(i)) \cdot r(i). \tag{5}$$

Finally, we can define our cost function for the pulsatility optimization as

$$c_{\text{pulse}} = c_{\text{virtual}} - c_{\text{real}}. \tag{6}$$

We use this cost function in the following optimization problem:

$$|c_{\text{pulse}}| \rightarrow \min. \tag{7}$$

We perform this optimization iteratively. Negative values for c_{pulse} indicate that the range in the simulated inflow velocity profile is too small to fit the measured data and should thus be increased. Positive values imply the opposite. For the first few iterations, the pulsatility is doubled/halved depending on the cost value c_{pulse}. After at least one positive and negative cost function value has been observed, we apply linear interpolation to estimate pulsatility at the zero cost value. Iteration is stopped when c_{virtual} is within 5% difference to the real amplitude c_{real}. The method yields stable numerical results and convergence is typically reached after three iterations.

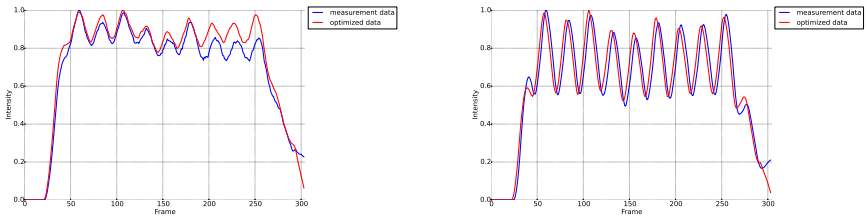

(a) Mean: 0.4 m/s, pulsatility: 0.1 m/s (b) Mean: 0.2 m/s, pulsatility: 0.2 m/s

Fig. 8 Comparison of time-intensity curves taken from synthetic data. The plots show the time-intensity curves that were measured in the input data and compare them to the final optimization result.

3 Evaluation and Results

Two different clinical cases were used to evaluate our approach. Both cases were acquired using the imaging protocol described in Section 2.1.

Synthetic Data For validation purposes, we generated several CFD simulations as ground truth data. The vasculature model was segmented from the 3D volumes of the 2 clinical data sets. Ground truth CFD simulations were then computed using these models and inflow profiles with a duration of 812 ms and varying settings for mean velocity (0.2 m/s – 0.4 m/s) and pulsatility (0.1 m/s – 0.2 m/s). We then used the described methods to estimate the specified ground truth parameters.

Figure 8 shows an example comparison of the observed synthetic time-intensity curves and the corresponding time-intensity curves resulting from the simulation with optimized boundary parameters. We observed an average error of approximately 5.7% ± 4.6% (mean ± standard deviation) for the mean velocity and 7.1% ± 11.4% for the pulsatility. The heart rate was estimated very precisely with an average error of about 0.8% ± 0.8%, which corresponds to about 6 ms error for the duration of one heart cycle. Lastly, we observed an error of about 11.7% ± 5.0% when synchronizing the heart state. While this error may seem relatively high, it corresponds to 71.7 ± 31.7 ms total offset, which represents a deviation of at most three projection frames.

Clinical Data Finally, we evaluated how well we can optimize the patient-specific boundary conditions using the real 3D time-resolved angiography data. For this evaluation, we rely on a comparison of the generated time-intensity curves, as no ground truth knowledge about the flow parameters was available.

This comparison of simulation results taken from real data is more difficult. The synthetic data we used for the previous evaluation only contained the simulated vessel segment. In real data, noise, brain parenchyma or small vessel branches which we did not consider in our reliability computation can lead an underlying low frequency in the measured time-intensity curves, which is not modeled in the simulation results. Figure 10 shows results of an optimization based on clinical data. On the right hand side we equalized the low frequency components of both signals, to make them more easily comparable.

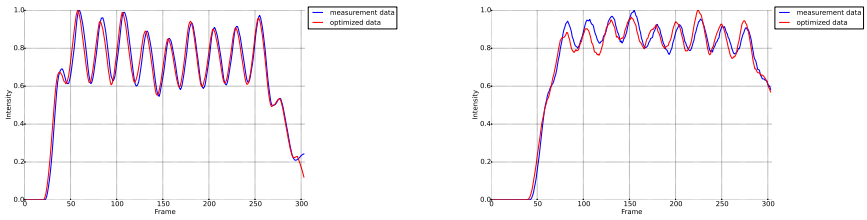

(a) Time-intensity curves at first centerline point.

(b) Time-intensity curves at last centerline point.

Fig. 9 Time-intensity curves taken from synthetic data with a mean velocity of 0.25 m/s and a pulsatility of 0.2 m/s. The plots show the time-intensity curves that were measured in the input data and compare them to the final optimization result. Curves measured at the first and last centerline point are shown.

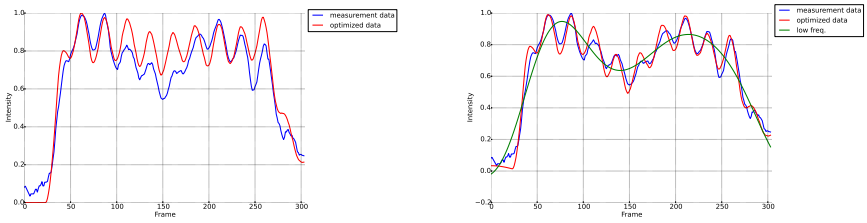

(a) Time-intensity curves from clinical data.

(b) With equalized low frequency components.

Fig. 10 Comparison of optimized time-intensity curves based on clinical data. The left plot show the time-intensity curves that were measured in the input data and compares them to the final optimization result. In 10(b) we set the low frequency components (also plotted) to the same values, in order to make the curves comparable.

4 Discussion and Conclusion

We presented an automatic workflow to generate patient-individualized CFD simulations (and virtual angiograms) based on time-resolved 3D rotational angiography data. The presented first evaluation based on two clinical cases shows that we are able to accurately estimate a patient's mean inflow velocity using a statistical approach. Using an iterative optimization that utilizes 3D CFD simulation as well as virtual angiography, we are further able to estimate the inflow velocities pulsatility with very high accuracy in about two to four iterations. We use a clinically available image acquisition protocol called 4D DSA, which requires only a single contrast agent injection to reconstruct the vessel geometry and provides temporal flow information at 30 frames per second. This has many benefits, as no registration of multiple datasets is required, and the patient is exposed to less contrast agent and less X-ray dose from independent acquisitions, as no additional 2D DSA images with high frame rates are required.

Disclaimer: The concepts and information presented in this paper are based on research and are not commercially available.

Conflict of interest: S. Gehrisch, T. Redel and M. Kowarschik are employees of Siemens Healthcare GmbH.
Ethical approval: This study has been performed retrospectively. Formal consent is not required.
Informed consent: For this type of study, formal consent is not required.

References

1. Bögel, M., Hölter, P., Redel, T., Maier, A., Hornegger, J., Dörfler, A.: A Fully-Automatic Locally Adaptive Thresholding Algorithm for Blood Vessel Segmentation in 3D Digital Subtraction Angiography. In: Engineering in Medicine and Biology Society (EMBC), 2015 37th Annual International Conference of the IEEE, pp. 2006–2009 (2015)
2. Bonnefous, O., Pereira, V., Ouared, R., Brina, O., H., A., Hermans, R., van Nijnatten, F., Stawiaski, J., Ruijters, D.: Quantification of arterial flow using digital subtraction angiography. Medical Physics **39**(10), 6264–6275 (2012)
3. Cebral, J.R., Radaelli, A., Frangi, A., Putman, C.M.: Qualitative comparison of intra-aneurysmal flow structures determined from conventional and virtual angiograms. In: Medical Imaging, pp. 65,111E–65,111E. International Society for Optics and Photonics (2007)
4. Davis, B., Royalty, K., Kowarschik, M., Rohkohl, C., Oberstar, E., Aagaard-Kienitz, B., Niemann, D., Ozkan, O., Strother, C., Mistretta, C.: 4D Digital Subtraction Angiography: Implementation and Demonstration of Feasibility. Am J Neuroradiol **34**(10), 1914–1921 (2013)
5. Durant, J., Waechter, I., Hermans, R., Weese, J., Aach, T.: Toward quantitative virtual angiography: Evaluation with in vitro studies. In: Biomedical Imaging: From Nano to Macro, 2008. ISBI 2008. 5th IEEE International Symposium on, pp. 632–635. IEEE (2008)
6. Endres, J., Kowarschik, M., Redel, T., Sharma, P., Mihalef, V., Hornegger, J., Dörfler, A.: A Workflow for Patient-Individualized Virtual Angiogram Generation Based on CFD Simulation. Computational and Mathematical Methods in Medicine **2012**(306765), 1–24 (2012)
7. Endres, J., Redel, T., Kowarschik, M., Hutter, J., Hornegger, J., Dörfler, A.: Virtual angiography using CFD simulations based on patient-specific parameter optimization. In: IEEE (ed.) International Symposium on Biomedical Imaging (ISBI), pp. 1200–1203 (2012)
8. Endres, J., Rohkohl, C., Schafer, S., Royalty, K., Maier, A., Kowarschik, M., Hornegger, J.: 4D DSA Iterative Reconstruction. In: M. King, S. Glick, K. Mueller (eds.) Proceedings of the Fully3D, pp. 276–279 (2015)
9. Ford, M.D., Stuhne, G.R., Nikolov, H.N., Habets, D.F., Lownie, S.P., Holdsworth, D.W., Steinman, D.: Virtual angiography for visualization and validation of computational models of aneurysm hemodynamics. Medical Imaging, IEEE Transactions on **24**(12), 1586–1592 (2005)
10. Gülsün, M., Tek, H.: Robust Vessel Tree Modeling. In: Medical Image Computing and Computer-Assisted Intervention - MICCAI 2008, pp. 602–611. Springer (2008)
11. Huang, T., Wu, T., Lin, C., Mok, G., Guo, W.: Peritherapeutic quantitative flow analysis of arteriovenous malformation on digital subtraction angiography. J Vasc Surg **56**(3), 812–815 (2012)
12. Karmonik, C., Klucnik, R., Benndorf, G.: Blood flow in cerebral aneurysms: comparison of phase contrast magnetic resonance and computational fluid dynamics-preliminary experience. Rofo **180**(3), 209–215 (2008)
13. Sun, Q., Groth, A., Bertram, M., Waechter, I., Bruijns, T., Hermans, R., Aach, T.: Phantom-based experimental validation of computational fluid dynamics simulations on cerebral aneurysms. Medical Physics **37**(9), 5054–5065 (2010)
14. Sun, Q., Groth, A., Waechter, I., Brina, O., Weese, J., Aach, T.: Quantitative evaluation of virtual angiography for interventional X-ray acquisitions. In: Biomedical Imaging: From Nano to Macro, 2009. ISBI '09. IEEE International Symposium on, pp. 895–898 (2009)
15. Wächter, I., Bredno, J., Hermans, R., Weese, J., Barrat, D., Hawkes, D.: Model-based blood flow quantification from rotational angiography. Medical Image Analysis **12**(5), 586–602 (2008)